Ballooning Instabilities in the Scrape-Off-Layer of Diverted Tokamaks as Giant ELM Precursors

R.A.M. Van der Linden, W. Kerner, O. Pogutse, B. Schunke.

Jet Joint Undertaking, Abingdon, Oxfordshire OX14 3EA, UK

ABSTRACT

The linear stability of the SOL to ballooning modes is studied using the reduced MHD model and applying the ballooning approximation to the perturbations. Particular attention is focused on the role of the X-point in the stability analysis and on the potential role of SOL ballooning instabilities as precursors to giant ELMs.

INTRODUCTION

The edge region of tokamaks is a main factor determining the macroscopic behaviour and performance characteristics of the entire plasma. Instabilities in the Scrape-off-Layer (SOL) are believed to generate micro-turbulence leading to enhanced transverse transport. Thus, a quantitative analysis of the stability of the SOL is crucial for understanding phenomena like the L-H transition and ELMs, and for determining the dependencies of quantities like the SOL width on the discharge parameters. In this paper, the stability of the SOL with respect to ballooning modes is studied. Since SOL field lines are open, the periodicity constraint that complicates the ballooning mode representation inside the separatrix is replaced by *`line-tying'* boundary conditions at the target plates. In the ideal MHD model applied here these target boundary conditions might be expected to exert a significant *stabilising influence*. However, on flux surfaces close to the separatrix the X-point effectively shields the plasma from the target plates and removes the stabilising effect. Since the *`magnetic well'* is strongly stabilising *inside* the separatrix and pressure gradients are very large just *outside* the separatrix, the SOL region may become unstable first, acting as a trigger to the release of energy from inside the separatrix.

MODEL

We use orthogonal flux coordinates (ρ, ω, φ) with metric $ds^2 = h_\rho^2 d\rho^2 + h_\omega^2 d\omega^2 + R^2 d\varphi^2$ to describe the magnetic field geometry near the separatrix. Using the reduced MHD equations and the eikonal representation for the perturbations [1]:

$$f(t,\rho,\omega,\varphi)=\tilde{f}(\rho,\omega)exp\left[\gamma t+in\int_{\omega_0}^{\omega}q(\rho,\omega')d\omega'-in\varphi\right],$$

with $nq >> 1$ yields the ballooning equation (here formulated in terms of the electric potential)

$$B_\varphi\left(\frac{B_\omega}{h_\omega B_\varphi}\frac{\partial}{\partial\omega}\right)\frac{1}{B_\varphi}\left(\frac{nq}{h_\omega}\right)^2\left(1+\zeta^2\right)\left(\frac{B_\omega}{h_\omega B_\varphi}\frac{\partial}{\partial\omega}\right)\tilde{\phi}-\gamma^2 c_A^{-2}\left(\frac{nq}{h_\omega}\right)^2\left(1+\zeta^2\right)\tilde{\phi}$$
$$-\frac{\mu_0}{RB_\varphi}\left(\frac{nq}{h_\omega}\right)^2\frac{1}{h_\rho}\left(\frac{1}{h_\rho}\frac{\partial}{\partial\rho}\frac{R}{B_\varphi}-\zeta\frac{1}{h_\omega}\frac{\partial}{\partial\omega}\frac{R}{B_\varphi}\right)\frac{dP_0}{d\rho}\tilde{\phi}=0,$$

where $q(\rho,\omega)=\dfrac{B_0 h_\omega}{B_\omega R}$ is the safety factor, and $\zeta(\rho,\omega,\omega_0)=\dfrac{h_\omega}{h_\rho}\dfrac{1}{q}\dfrac{\partial}{\partial\rho}\int_{\omega_0}^{\omega}q d\omega'$ is the shear. We can apply the model to an experimental configuration, or use an analytical two-wire current model which allows high accuracy and makes it possible to separate individual effects. The metric coefficients and magnetic field in the (straight) two-wire model are given by:

$$h_\rho^2=h_\omega^2=h^2=\frac{y_0^2}{4}\frac{exp(2\rho)}{\left[1-2exp(\rho)cos(\omega)+exp(2\rho)\right]^{1/2}},$$

$$B_\omega(\rho,\omega)=\frac{B_{\omega 0}(\rho)}{h_\omega R},\qquad B_\varphi(\rho,\omega)=\frac{B_{\varphi 0}R_0}{R}.$$

The separatrix is located at $\rho=0$, while the X-point is given by $\omega=0,2\pi$. We define the dimensionless quantities

$$\tilde{\beta}=\frac{\mu_0}{B_{\varphi 0}^2}\frac{dp_0}{d\rho}\qquad\text{and}\qquad S_0=\frac{1}{q(\rho,\pi)}\frac{\partial}{\partial\rho}q(\rho,\pi).$$

Qualitatively, the results obtained for the experimental configuration and for the analytical model are very similar. This is illustrated in figures 1 and 2, where the (dimensionless) growth rate is plotted as a function of ω_0 for typical cases.

The strong variation of the growth rates near the X-point reflects the strong variation of the equilibrium quantities. The characteristic feature that *identical* maximum growth rates are found at three points (one near the midplane and one on each side of the X-point) is due to the non-monotonic behaviour of $\int\frac{\partial q}{\partial\rho}$, as explained in detail in Kerner et al. (1996) [2].

STABILITY ANALYSIS OF THE EDGE REGION IN JET DISCHARGES

Experimentally it has been found that the duration of the ELM-free period can be increased by stronger shaping of the magnetic configuration, as shown in figure 3. This agrees with the higher critical gradient for the ballooning instability displayed in figure 4. It is also clear from figure 4 that $\tilde{\beta}_{crit}$ is lower in the SOL than inside the separatrix.

STABILITY ANALYSIS OF A TWO-WIRE MODEL OF THE SEPARATRIX REGION

In figure 5 the influence of shear on the marginal stability point $\tilde{\beta}_{crit}$ is shown. For small values of ρ we find the linear dependence $\tilde{\beta}_{crit} = a(S_0) + \rho b(S_0)$. Close to the separatrix shear is stabilising, but further out the dependence becomes non-monotonic. Thus the global effect of shear depends strongly on the natural mode width (e.g. due to FLR effect). Not shown here is that shear also affects the position where the most unstable solution is found. When the height of the X-point is varied (keeping the configuration fixed but increasing the distance of the target plates) it is found that close to the separatrix the height of the X-point has no significant effect on the critical gradient, i.e. the target plates are effectively shielded by the X-point (see Kerner et al. for more details). The eigenfunctions indicate that the perturbations of physical quantities (e.g. $\delta B_\rho \sim \frac{\partial^2 \phi}{\partial \omega^2}$, $\delta v_\rho \sim \frac{\partial \phi}{\partial \omega}$) are localised near the X-point.

DISCUSSION

We have shown that the critical gradient for ideal ballooning modes in the SOL is lower than that just inside the separatrix. The X-point has a strong influence on the stability of the SOL (mainly by shielding the upstream plasma from the target plates), and in particular we have found that the perturbations of physical quantities are localised near the separatrix in the X-point region (some localisation near the midplane is also possible). The effect of shear is generally stabilising for modes that are strongly localised (i.e. with narrow mode width), but for larger mode widths shear may destabilise instead. The stability characteristics of the tokamak edge region are compatible with the ELM model proposed by Pogutse et al. [3]. In this model, the ballooning instability in the SOL is conjectured to act as precursor for giant ELMs. Because of the localisation the ballooning instability in the SOL destroys the magnetic X-point geometry and this makes hot plasma from inside the separatrix come into contact with the wall. The thus generated impurity influx then triggers the instability inside the separatrix (the main macroscopic event). Finally, the expelled plasma layers are diffusively refilled. This model leads to an estimate for the ELM frequency

$$f \propto \frac{P_{in} B_0}{I^3 \Delta_P^{1/2}}$$

As shown in figure 6, the predicted linear dependence on input power agrees with the experiment. An inverse dependence on input power is also obvious, but the exact scaling needs to be further investigated.

REFERENCES

[1] J. Connor, R. Hastie, and B. Taylor, Proc. R. Soc. (London). Ser. A365 (1979) 1.

[2] W. Kerner, O. Pogutse, R.A.M. Van der Linden and B. Schunke, submitted to Plasma Physics and Controlled Fusion.

[3] O. Pogutse, J.C. Cordey, W. Kerner, and B. Schunke, Proc. 22nd EPS Conf. on Controlled Fusion and Plasma Physics (Bournemouth, 1995), Vol III p.277.

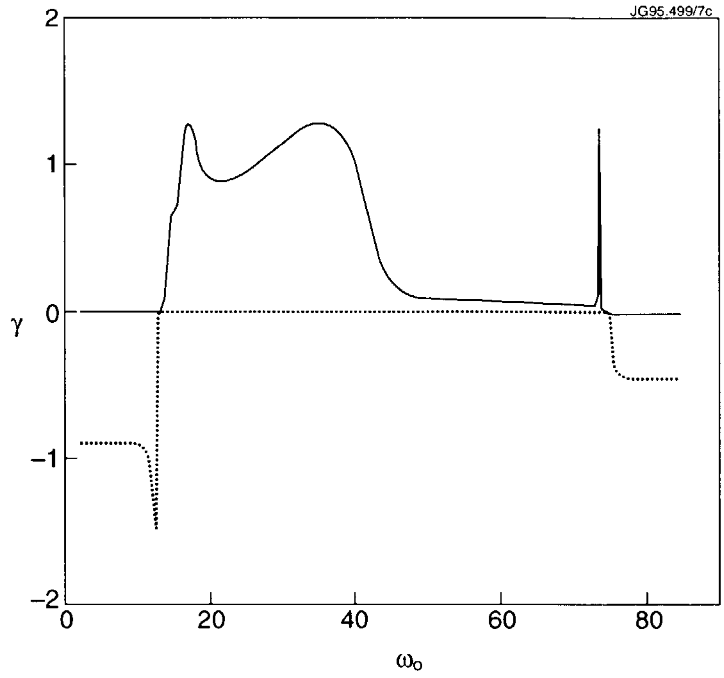

Fig.1: Growth rates for JET experimental configuration (pulse 31300).

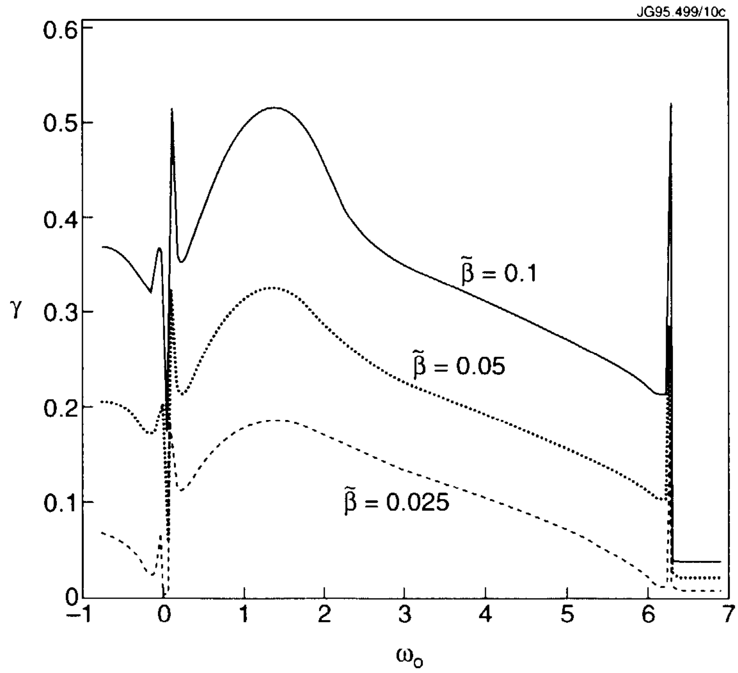

Fig.2: Growth rates for analytical model (S_0=0).

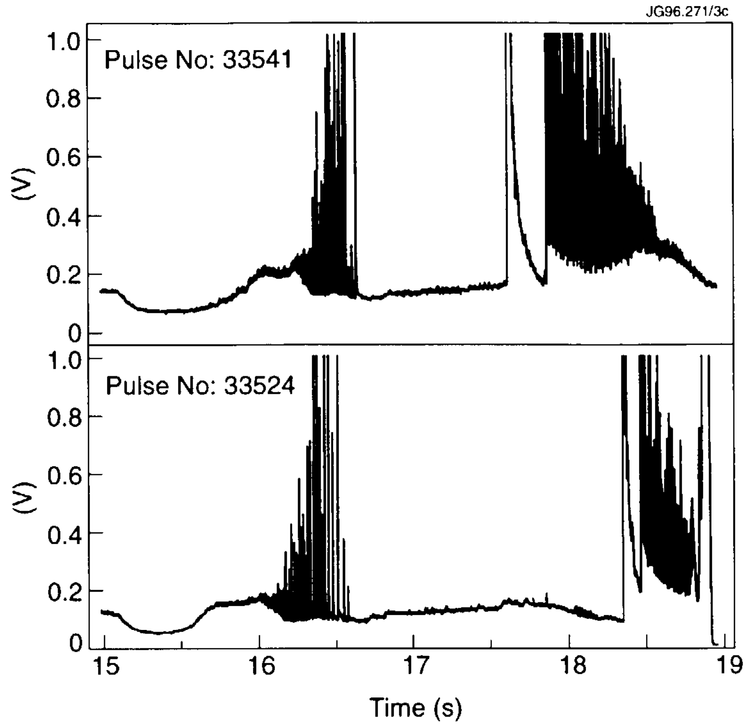

Fig. 3: Elm behaviour of two discharges with different shaping (D_α signal).

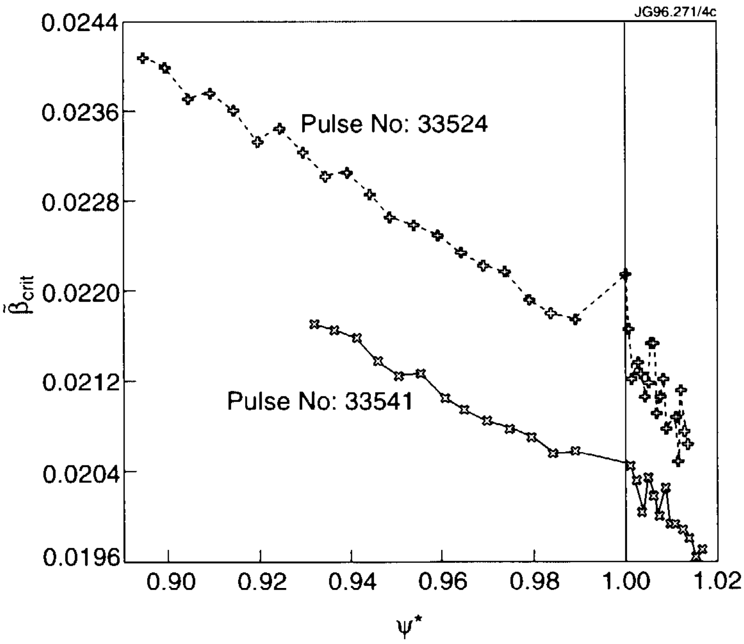

Fig. 4: Calculated $\tilde{\beta}_{crit}$ for these discharges

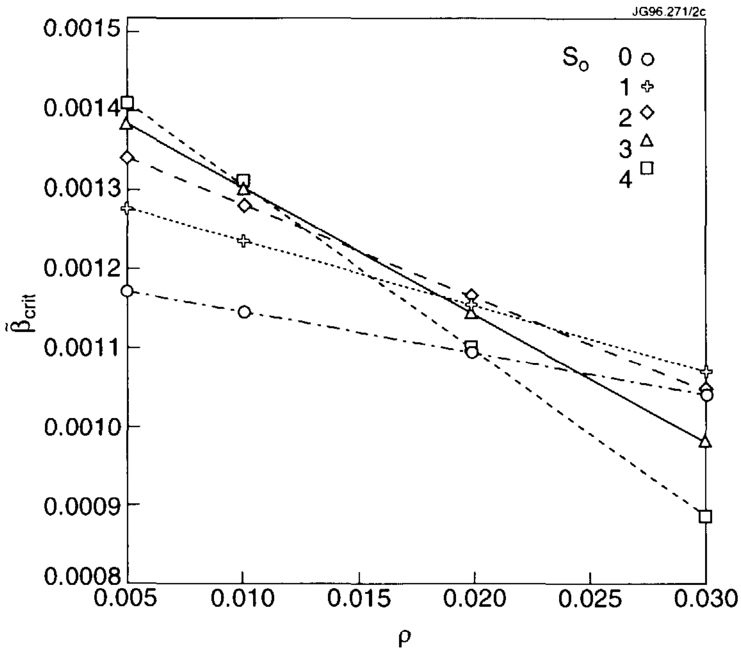

Fig. 5 Dependence of $\bar{\beta}_{crit}$ on shear S_o

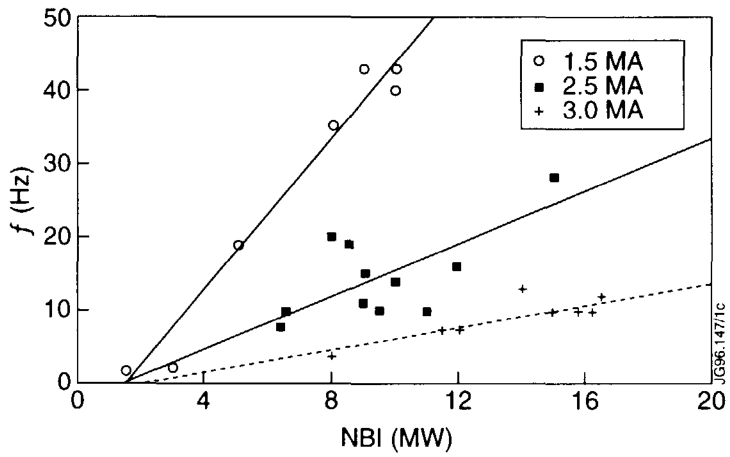

Fig. 6 Experimental dependence of ELM frequency on input power.